The ROI CT problem: a shearlet-based regularization approach

Tatiana A. Bubba[1], F. Porta[2], G. Zanghirati[2] and S. Bonettini[2]

[1]Dept. of Physics, Comp. Sci. and Maths, University of Modena and Reggio Emilia, Italy, and INdAM-GNCS
[2]Dept. of Maths and Comp. Sci., University of Ferrara, Italy, and INdAM-GNCS

tatiana.bubba@unimore.it, {federica.porta, g.zanghirati, silvia.bonettini}@unife.it

OASIS Optimization Algorithms and Software for Inverse problemS

http://www.oasis.unimore.it/

Goal and Motivations

Health hazards for patients due to ionizing radiations in Computed tomography (CT) can be reduced by limiting the irradiation to a subregion of the object to be reconstructed, the so-called *region-of-interest* (ROI). The goal is to obtain a stable reconstruction of the ROI without any assumption either on the size or the location of the ROI, overcoming the ill-posedness of the problem and the instability of naive local reconstruction algorithms.

State of the art

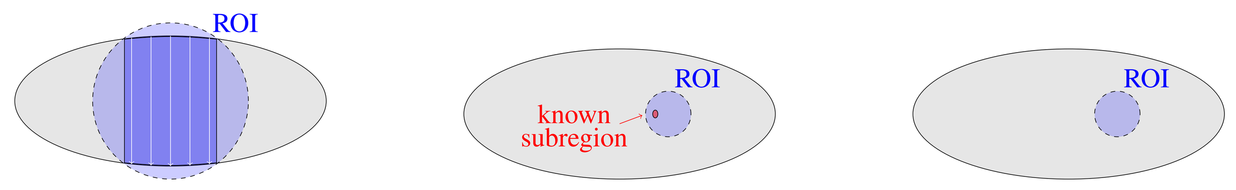

(a) (b) (c)

Examples of recoverable regions:

(a) from (at least) one projection view the object is completely recovered;

(b) a known subregion inside the ROI is given;

(c) no assumption either on the size or on the location of the ROI, except for its convex shape.

2D problem setting

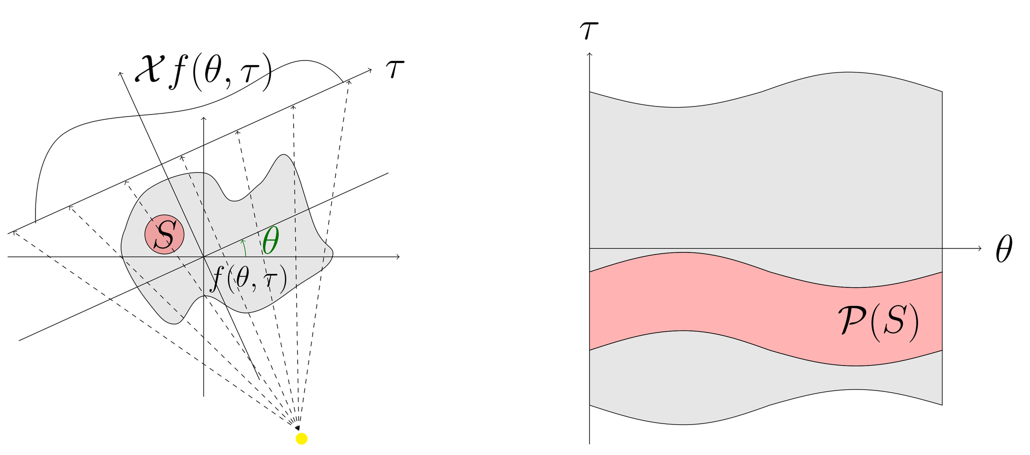

The aim of ROI CT is to reconstruct an integrable function f from its X-ray projections y_0 known only within a subregion inside the FOV, while the rest of the image is ignored. This is accomplished by setting:

$$y_0(\theta,\tau) = M(\theta,\tau)\,\mathcal{X}f(\theta,\tau)$$

where

$$\mathcal{X}f(\theta,\tau) = \int_{\ell(\theta,\tau)} f(\mathbf{x})\,d\mathbf{x} = \int_{\mathbb{R}^2} \delta(\tau - \mathbf{x}\cdot e_\theta)\,f(\mathbf{x})\,d\mathbf{x}$$

is the *X-ray transform* of f at (θ,τ) and the mask M identifies the ROI S in the sinogram space

$$M(\theta,\tau) = 1_{\mathcal{P}(S)}(\theta,\tau).$$

Given y_0 defined on $\mathcal{P}(S)$, the goal is to extrapolate it to the region outside $\mathcal{P}(S)$, ensuring that the X-ray projections $y = \mathcal{R}f$ comes from the X-ray transform of a function $f \in L^1 \cap L^2$:

$$M\mathcal{R}f = My = y_0 \qquad \text{(data fidelity)}$$
$$(1-M)\mathcal{R}f = (1-M)y \qquad \text{(data consistency)}$$

2D discrete setting

Denoting with $\mathbf{W}$ the $N_\theta N_{\text{dtc}} \times N^2$ forward projection matrix, the data fidelity and consistency equations read as follows:

$$\mathbf{MWf} = \mathbf{My} = \mathbf{y_0} \qquad \text{(data fidelity)}$$
$$(\mathbf{I}_{N_\theta N_{\text{dtc}}} - \mathbf{M})\,\mathbf{Wf} = (\mathbf{I}_{N_\theta N_{\text{dtc}}} - \mathbf{M})\,\mathbf{y} \qquad \text{(data consistency)}$$

where N_θ = # projection angles, N_{dtc} = # detector elements, N = width in pixel of the reconstructed object.

Unfortunately, these equations alone do not lead to a unique solution [5]. A suitable one can be derived by using regularization:

$$\hat{\mathbf{f}} = \operatorname*{argmin}_{\mathbf{f}\in\mathbb{R}^{N^2}} \mathbf{\Psi}(\mathbf{f})$$

where

$$\mathbf{\Psi}(\mathbf{f}) = \frac{1}{2}\|\mathbf{MWf} - \mathbf{y_0}\|_2^2 + \lambda\,\|\mathbf{\Phi}((\mathbf{I}_{N_\theta N_{\text{dtc}}} - \mathbf{M})\mathbf{Wf} + \mathbf{y_0})\|_p^p + \iota_{\Omega_\mathbf{f}}.$$

Here, λ is a regularization parameter; $\iota_{\Omega_\mathbf{f}}$ is the indicator function of the feasible region $\Omega_\mathbf{f}$, which is defined as $\mathbf{f} \geq 0$ or $0 \leq \mathbf{f} \leq L$, where L is the image maximum pixel intensity; Φ is the shearlet (or wavelet) transform matrix [6], and $p = 2$ or $p = 1$.

Distance-Driven method

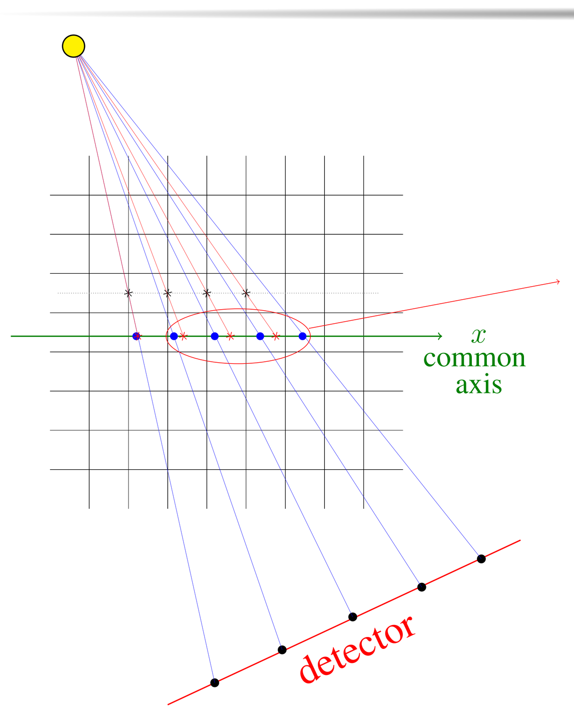

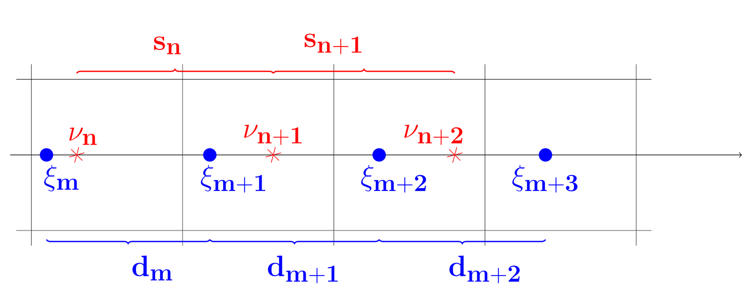

Each object pixel (voxel) and detector cell is mapped onto a common axis (plane) by its projecting boundary midpoints:

$$d_{m+1} = \frac{\nu_{n+1} - \xi_{m+1}}{\xi_{m+2} - \xi_{m+1}} s_n + \frac{\xi_{m+2} - \nu_{n+1}}{\xi_{m+2} - \xi_{m+1}} s_{n+1}$$

The length of the overlap is used as projection weight.

There are two main ingredients [4]:

- kernel operation:

$$d_m = \sum_n w_{m,n} s_n \qquad \text{with} \qquad w_{m,n} = \frac{\left[\min(\xi_{m+1},\nu_{n+1}) - \max(\xi_m,\nu_n)\right]_+}{\xi_{m+1} - \xi_m}, \qquad [x]_+ = \max(x,0)\,,$$

- there is a (possibly zero) length of overlap between each image pixel and each detector cell due to the bijection between the position on the detector and the position within an image row (or column).

Advantages:

- Low computational cost and highly sequential memory access patterns
- Avoids artifacts (*e.g.*, due to interpolation) of classical methods

Variable metric inexact line-search algorithm

VMILA belongs to the class of proximal-gradient methods [1]. Main features:

- Designed for problem of the form $\min_{x\in\mathbb{R}^n} g(x)$ where

$$g(x) = g_0(x) + g_1(x)$$

  with g_1 is convex, possibly nonsmooth, and g_0 is smooth, possibly non-convex. This formulation includes also constrained problems over convex sets.
- descent direction based on the proximal operator associated to the convex part of the objective function

$$\text{prox}_{g_0}(x) = \arg\min_{z\in\mathbb{R}^n} g_0(z) + \frac{1}{2}\|z - x\|^2 \qquad \forall\, x \in \mathbb{R}^n$$

- Armijo-like rule to determine the step size along the descent direction
- adaptive step-length selection (BB-like updating rules)

Numerical results

$\sigma = 0.05$

	$\mathbf{r}_{\text{ROI}} = 0.25N$ iter	value	sec	$\mathbf{r}_{\text{ROI}} = 0.15N$ iter	value	sec	$\mathbf{r}_{\text{ROI}} = 0.1N$ iter	value	sec
ROI PSNR									
Sm	83	35.86	4.7	109	33.61	6.0	106	32.57	5.8
NSm	83	36.94	15.1	78	41.98	14.2	48	45.43	8.6
ROI Relative error									
Sm	83	0.21	4.7	109	0.57	6.0	106	1.06	5.8
NSm	83	0.19	15.1	78	0.22	14.2	48	0.24	8.6

$\sigma = 0.1$

	$\mathbf{r}_{\text{ROI}} = 0.25N$ iter	value	sec	$\mathbf{r}_{\text{ROI}} = 0.15N$ iter	value	sec	$\mathbf{r}_{\text{ROI}} = 0.1N$ iter	value	sec
ROI PSNR									
Sm	77	35.49	5.3	111	35.37	7.6	102	37.12	6.9
NSm	48	37.76	10.5	72	40.92	15.9	62	44.64	13.6
ROI Relative error									
Sm	77	0.23	5.3	111	0.46	7.6	102	0.63	6.9
NSm	48	0.17	10.5	72	0.25	15.9	62	0.26	13.6

Optimal results, with respect to PSNR and relative error, for p=2 (Sm) and p=1 (NSm), and λ=10^{-4}.

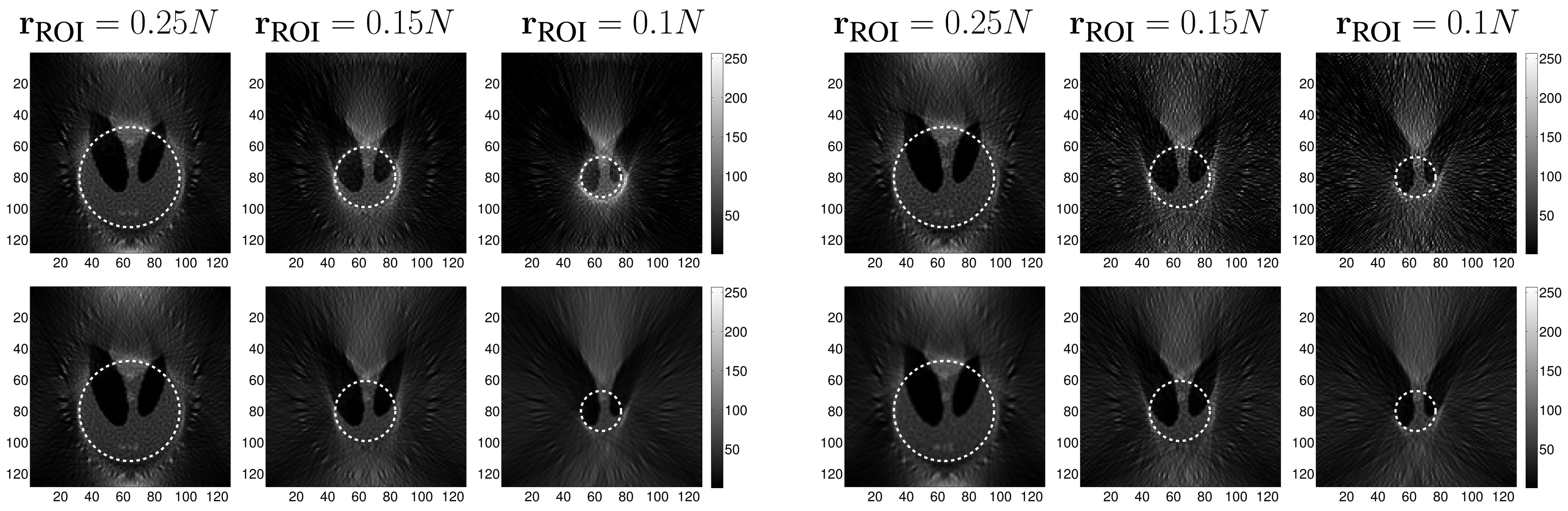

Optimal reconstructions of the Shepp-Logan phantom, sized 128×128, for decreasing radii.
First row: smooth formulation ($p = 2$). Second row: nonsmooth formulation ($p = 1$).
Noise: white Gaussian process, with zero mean and variance $\sigma = 0.05$ (left) or $\sigma = 0.1$ (right).

Conclusions and Forthcoming Research

- Accurate ROI reconstructions are recovered regardless of the location and size of the ROI, and for rather small ROI sizes
- Nonsmooth approach performs better: 1-norm suppresses smaller shearlet coefficients in favor of few larger shearlet coefficients, associated to edges
- Slightly better reconstructions can be obtained by exploiting a smooth TV approach. However, this is strongly dependent on the phantom features and may not hold for more general (real) data.

Future perspectives:

- Obtain stable reconstructions from Poisson noisy data and real data
- Apply the same machinery to helical CT

Acknowledgements

This work is supported by INdAM-GNCS, the Italian national research project FIRB2012, grant n. RBFR12M3AC, FAR2014-UniFE and FAR2014-UniMORE.

References

[1] S. Bonettini, I. Loris, F. Porta, and M. Prato. Variable metric inexact line-search based methods for nonsmooth optimization. *SIAM J. Optim.*, 26(2):891–921, 2016.

[2] T.A. Bubba, D. Labate, G. Zanghirati, and S. Bonettini. Numerical assessment of shearlet-based regularization in ROI tomography. *ArXiv e-prints 1511.04336*, nov 2015.

[3] T.A. Bubba, D. Labate, G. Zanghirati, S. Bonettini, and B. Goossens. Shearlet-based regularized ROI reconstruction in fan beam computed tomography. In *SPIE Optics & Photonics, Wavelets And Applications XVI*, volume 9597, page 95970K, San Diego, CA, USA, Aug 10-12 2015.

[4] B. De Man and S. Basu. Distance-driven projection and backprojection in three dimensions. *Physics in Medicine and Biology*, 7:2463–75, 2004.

[5] B. Goossens, D. Labate, and B. Bodmann. Region-of-interest computed tomography by regularity-inducing convex optimization. *Private communication*, 2016.

[6] G. Kutyniok and D. Labate. *Shearlets. Multiscale Analysis for Multivariate Data*. Birkhäuser, Boston, MA (USA), 2012.

[7] B. Vandeghinste, B. Goossens, R. Van Holen, C. Vanhove, A. Pižurica, S. Vandenberghe, and S. Staelens. Iterative CT reconstruction using shearlet-based regularization. *IEEE Trans. Nuclear Science*, 5:3305–17, 2013.